Published as: *Nature*. 2013 January 24; 493(7433): 537–541.

Dopamine neurons modulate neural encoding and expression of depression-related behaviour

Kay M. Tye[#1,2], **Julie J. Mirzabekov**[#2], **Melissa R. Warden**[#2], **Emily A. Ferenczi**[2,3], **Hsing-Chen Tsai**[2,3], **Joel Finkelstein**[2], **Sung-Yon Kim**[2,3], **Avishek Adhikari**[2], **Kimberly R. Thompson**[2], **Aaron S. Andalman**[2], **Lisa A. Gunaydin**[2], **Ilana B. Witten**[2], and **Karl Deisseroth**[2,3,4,5,6]

[1]Picower Institute for Learning and Memory, Brain and Cognitive Sciences, Massachusetts Institute of Technology, Cambridge, Massachusetts 02139, USA.

[2]Department of Bioengineering, Stanford University, Stanford, California 94305, USA.

[3]Neurosciences Program, Stanford University, Stanford California 94305, USA.

[4]Department of Psychiatry and Behavioral Sciences, Stanford University, Stanford, California 94305, USA.

[5]Howard Hughes Medical Institute, Stanford University, Stanford California 94305, USA.

[6]CNC Program, Stanford University, Stanford, California 94305, USA.

[#] These authors contributed equally to this work.

Abstract

Major depression is characterized by diverse debilitating symptoms that include hopelessness and anhedonia[1]. Dopamine neurons involved in reward and motivation[2–9] are among many neural populations that have been hypothesized to be relevant[10], and certain antidepressant treatments, including medications and brain stimulation therapies, can influence the complex dopamine system. Until now it has not been possible to test this hypothesis directly, even in animal models, as existing therapeutic interventions are unable to specifically target dopamine neurons. Here we investigated directly the causal contributions of defined dopamine neurons to multidimensional depression-like phenotypes induced by chronic mild stress, by integrating behavioural, pharmacological, optogenetic and electrophysiological methods in freely moving rodents. We found that bidirectional control (inhibition or excitation) of specified midbrain dopamine neurons immediately and bidirectionally modulates (induces or relieves) multiple independent depression

Correspondence and requests for materials should be addressed to K.M.T. (kaytye@mit.edu) and K.D. (deissero@stanford.edu)..

Supplementary Information is available in the online version of the paper.

Author Contributions K.M.T., J.J.M., M.R.W., H.-C.T. and K.D. contributed to study design. K.M.T., J.J.M., M.R.W., H.-C.T., J.F., S-Y.K., E.A.F., A.A., K.R.T., L.A.G., I.B.W. and K.D. contributed to data collection or interpretation. K.M.T. coordinated all experiments, M.R.W. led development of the induction-coil FST and the FST electrophysiology; K.M.T., J.J.M., M.R.W. and A.S.A. contributed to data analysis, and K.D. supervised the project. K.M.T. and K.D. wrote the paper.

Author Information Reprints and permissions information is available at www.nature.com/reprints. The authors declare competing financial interests: details are available in the online version of the paper. Readers are welcome to comment on the online version of the paper.

symptoms caused by chronic stress. By probing the circuit implementation of these effects, we observed that optogenetic recruitment of these dopamine neurons potently alters the neural encoding of depression-related behaviours in the downstream nucleus accumbens of freely moving rodents, suggesting that processes affecting depression symptoms may involve alterations in the neural encoding of action in limbic circuitry.

Major depressive disorder is a debilitating disease characterized by diverse symptoms that include depressed mood, suicidality, psychomotor retardation or agitation, reduced motivation or hopelessness, and anhedonia[1]. Current medical therapies for depression take weeks to achieve full efficacy, and are ineffective in many patients or cause intolerable side effects, pointing to the need for deeper understanding of depression states and treatment. Given that there is strong evidence linking the mesolimbic dopamine system with reward-related[2,3], hedonic[4–6] and motivated[7–9] behaviours, we proposed to test whether midbrain dopamine neurons could have a causal role in both induction and relief of diverse stress-induced depression-related behaviours[10], including reduced motivation and anhedonia[4,8,10,11]. To test this, we developed and used an array of tools for real-time assessment and control of depression-related states in freely moving rodents.

We first tested whether selective inhibition of ventral tegmental area (VTA) dopamine neurons could acutely induce multiple depression-like behaviours. We expressed an enhanced halorhodopsin that hyperpolarizes neuronal membranes upon illumination (eNpHR version 3.0; eNpHR3.0) in VTA tyrosine hydroxylase (TH)-expressing dopamine neurons, by injecting a Cre-dependent adeno-associated virus (AAV) carrying this eNpHR3.0 into the VTA of TH::Cre mice[6] (Fig. 1a and Supplementary Fig. 1). eNpHR3.0 was fused to the enhanced yellow fluorescent protein (eYFP) so that targeting specificity could be tracked by quantifying the proportion of VTA neurons expressing eNpHR3.0–eYFP (or eYFP alone in age-matched controls) that were also TH-positive (Fig. 1b and Supplementary Fig. 2).

Primary categories of depression assays in rodents involve well-validated tests of motivation and anhedonia[12–15] in which performance degrades with chronic stress and improves with chronic antidepressantmedication treatment[13,15]. In the context of depressive phenotypes, motivation is assayed by presenting rodents with an inescapable stressor, such as those used in the tail-suspension test (TST) or forced-swim test (FST), and quantifying the proportion of time spent performing escape-related behaviour (struggling) relative to time spent immobile, which has been interpreted as a sign of behavioural despair or passivity[12]. Here we compared mice with VTA dopamine neurons expressing eNpHR3.0 to eYFP-expressing controls, and observed a significant and reversible reduction in escape-related behaviour upon illumination (Fig. 1c). We investigated whether this reduction in struggling was related to a gross locomotor effect, rather than a more selective decrease in motivation to escape, by evaluating inhibition of VTA dopamine neurons in these same animals during exploration of an open-field-test (OFT) arena. There was no significant difference in locomotion between groups (Fig. 1d and Supplementary Figs 3 and 4). Although no difference was detected, any trend towards subtly decreased locomotion in the eNpHR3.0 group upon illumination in the OFT would still be consistent with a depression-related phenotype, given that related motor

changes are clinically observed as psychomotor retardation and/or reduced motivation to explore (Supplementary Information).

We next developed a temporally precise version of an assay for anhedonia, the sucrose-preference test[13,14]. We quantified (by automated detection) the number of licks on spouts delivering either water or 1% sucrose during a 90-min session consisting of a baseline 30-min light-off epoch, followed by a 30-min light-on epoch, and ending with another 30-min light-off epoch (Fig. 1e and Supplementary Fig. 5a). Notably, we observed a significant reduction in sucrose preference during illumination in eNpHR3.0 mice but not eYFP control mice (Fig. 1e), and no significant group-by-epoch interaction (two-way analysis of variance (ANOVA)) in total licks (Supplementary Fig. 5a). Therefore, optogenetic inhibition of VTA dopamine neurons defined a phenotype that could be immediately induced and reversed, and that was consistent with multiple depression-symptom categories of behavioural despair and anhedonia[12].

To test for a causal link to existing depression-like states, we also probed the ability of dopamine-neuron activation to correct independent depression-like phenotypes induced by stress[4]. As clinical depression can be linked to stressors operating over months, we used the time-intensive chronic mild stress (CMS) paradigm in which unpredictable mild stressors are delivered twice daily for 8 to 12 weeks to induce a depressive-like state[13]. CMS has been shown to produce decreases in motivation, assayed by reduction in escape-related behaviour in the face of inescapable stressors, as well as anhedonia, as measured by reduced sucrose preference[12–14].

To phasically activate VTA dopamine neurons, we selectively expressed channelrhodopsin-2 (ChR2) in these cells to achieve temporally precise excitation with light. We included four groups of mice (Fig. 2a and Supplementary Fig. 6): mice with ChR2-transduced VTA dopamine neurons and exposed to CMS; mice with eYFP-transduced VTA dopamine neurons and exposed to CMS; mice with ChR2-transduced VTA dopamine neurons and housed in a low-stress environment (non-CMS); and mice with eYFP-transduced VTA dopamine neurons and non-CMS.

We examined animals during baseline (light-off), phasic illumination (light-on) and post-illumination (light-off) epochs (Fig. 2b) during multiple behavioural assessments. To produce phasic firing in VTA dopamine neurons, we used a physiological, sparse bursting illumination pattern (Fig. 2b; 8 pulses at 30 Hz, 5-ms pulse width, every 5 s) similar to patterns known to elicit phasic spiking and dopamine transients[6] during illumination epochs. To assess behavioural motivation we exposed all four groups of animals to the TST. At baseline, consistent with previous studies[15], we observed (Fig. 2c) that CMS markedly reduced the amount of escape-related behaviour relative to non-CMS controls by approximately 50%; moreover, upon illumination, the ChR2-CMS group showed a robust increase in escape-related behaviour, relative to the eYFP-CMS group ($P < 0.001$). Thus, phasic illumination of VTA dopamine neurons in ChR2 CMS mice, but not eYFP CMS mice, reversed the CMS-induced depression-like phenotype back to non-CMS levels, with timing on the order of seconds (Fig. 2c).

As dopamine neurons in some systems are linked to locomotion[9], we examined locomotion in the OFT chamber (of the same mice included in the TST assay) during two 3-min light-on epochs, interleaved with two 3-min light-off epochs using the same phasic illumination parameters described above (Fig. 2d). On the timescale corresponding to TST effects, only statistically non-significant interactions with altered OFT velocity were observed in ChR2 groups upon illumination.

Next, we tested whether phasic activation of VTA dopamine neurons could also reverse CMS-induced decreases in sucrose preference (Fig. 2e). Consistent with previous studies, baseline measurements showed that eYFP and ChR2 CMS mice expressed significantly lower sucrose preference than eYFP and ChR2 non-CMS mice before illumination on the lickometer assay (Bonferroni post-hoc tests, $P < 0.05$ and $P < 0.01$, respectively). However, phasic activation of VTA dopamine neurons acutely reversed the CMS-induced anhedonic effect in ChR2 CMS, but not eYFP CMS, animals (Fig. 2e) without altering the total number of licks across groups (Supplementary Fig. 5b).

Together these results show bidirectional effects of VTA dopamine neuron activity on rapidly inducing and ameliorating diverse depression-related behaviours. We next considered how chronic mild stress itself might influence VTA neuronal activity. To investigate this, we recorded from the VTA of CMS ($n = 93$ neurons) or non-CMS ($n = 71$ neurons) animals to probe neuronal firing properties (Supplementary Figs 8–10). The mean spike rate was maintained between groups, but out of the total spikes recorded, VTA neurons in non-CMS rats had a significantly greater proportion of spikes occurring within bursts, had longer-duration bursts, and had more spikes in each burst compared to VTA neurons in CMS rats (Supplementary Fig. 9), indicating that CMS alters normal bursting activity.

As VTA dopamine neurons project to multiple regions throughout the brain[16], it is not clear which downstream targets may be contributing to the changes in depression-related behaviours, although it is perhaps relevant that clinical deep brain stimulation in the NAc (among other targets) has been proposed to modulate depression-related symptoms[17]. Since the NAc does receive (among many other inputs) dopaminergic innervation *in vivo* that can guide certain motivated behaviours[5] and glutamatergic innervation involved in reward-related conditioning, we next tested whether glutamate or dopamine transmission in the NAc could mediate the light-induced rescue of the depression-like phenotype, using mice that were implanted with bilateral guide cannulae in the NAc in the setting of viral ChR2 transduction of VTA dopamine neurons and chronic implantation of a fibre-optic cable targeted at the VTA (Supplementary Figs 11 and 12), before undergoing 8 to 12 weeks of CMS.

We carried out within-subject comparisons counter-balanced for order, and infused either saline, or glutamate-receptor antagonists, into the NAc before the TST. Glutamate-receptor antagonism did not attenuate the light-induced reversal of reduced struggling following CMS seen, but instead increased overall struggling (Supplementary Fig. 11a). As the NAc receives glutamatergic innervation from many regions, we speculate that the net effect of these inputs may suppress struggling in the TST, perhaps consistent with acute clinical anti-

depressant effects of the much more broadly acting systemic drug ketamine[18]. In contrast, in a second within-subject comparison, we found that dopamine-receptor blockade in the NAc reduced baseline struggling and blocked the light-induced reversal of reduced struggling following CMS (Supplementary Fig. 11b). These findings are consistent with the hypothesis that dopaminergic innervation from the VTA to the NAc is important for maintaining baseline levels of motivated escape behaviour as well as for elevations in this behaviour elicited by phasic activity of VTA dopamine neurons.

Together, these data have shown that selective inhibition of VTA dopamine neurons acutely produces depression-related behaviour in measures of both motivation and anhedonia, and that phasic activation of VTA dopamine neurons acutely rescues a chronic mild stress-induced depression-like phenotype, in a phenomenon that requires functioning of dopamine receptors in the NAc. Next, to investigate high-temporal resolution neural representations of depression-related action in downstream neurons under baseline and phasic activation conditions of VTA dopamine neurons, we combined several new tools. Although the sucrose-preference task is not suited for high-temporal resolution assessment of neural representations of behaviour, as the outcome is manifested slowly and stochastically over many tens of minutes, we considered that escape-related behaviour might be better suited for simultaneous circuit-dynamics measurement. However, FST quantification traditionally involves low temporal-resolution annotation of immobility epochs. We required a new method for millisecond-temporal-resolution detection of escape-related behaviour for integration with optogenetics and *in vivo* electrophysiology.

Because even a lightweight electrophysiological recording headstage impeded normal escape-related behaviours in mice, this experiment required TH::Cre rats[3], which were able to express escape-related behaviours while bearing an electrophysiological recording headstage in the FST without mechanical noise (Fig. 3a–c). We used a novel high-speed method of magnetic induction-based assessment of depression-related behaviour, placing a magnetic coil surrounding the forced-swim tank and a small magnet attached to the hind-paw to measure swimming kicks or escape-related behaviour. We validated that illumination of ChR2-expressing VTA dopamine neurons in TH::Cre rats rapidly and reversibly increased escape-related behaviour (Fig. 3 and Supplementary Fig. 13) but did not alter locomotion in the OFT (Fig. 3d and Supplementary Fig. 14).

We carried out *in vivo* electrophysiological recordings in the NAc of TH::Cre rats[3] during baseline activity in the home cage, during exploration in the OFT, and during the FST (Fig. 3a and Supplementary Fig. 15) while illuminating ChR2-expressing VTA dopamine neurons following CMS (Fig. 3b, c). We observed a robust increase in kick frequency during light-on epochs relative to light-off epochs, but did not observe time-locked kicking to light pulses on the order of seconds (Fig. 3c–e), suggesting that this behaviour may be modulated by dopaminergic tone rather than individual dopamine transients. We also found that the more NAc neurons showing phasic responses to VTA dopamine activation in an animal, the greater the relative increase in escape-related behaviour, but not OFT locomotion (Supplementary Fig. 16 and Fig. 3f).

We examined the proportion of NAc neurons (n = 123) showing phasic responses to light pulses in VTA or phasic responses associated with FST kicks (Supplementary Figs 17 and 18). Many NAc neurons (45 out of 123 (37%); Fig. 4a) showed phasic responses to VTA light (see Supplementary Materials for statistical methods). Of these 45 neurons, 6 showed phasic inhibition to light, whereas the dominant population (39 out of 45) showed phasic excitation. Separate from phasic responses, we also observed that upon FST exposure, more NAc neurons showed decreases than increases in mean epoch firing rate compared with home-cage firing (Supplementary Fig. 19). Furthermore, 49 out of 123 NAc neurons (40%; Fig. 4a) encoded escape-related behaviour, as seen by phasic responses associated with kick events; 14 of these 49 (29%) showed phasic inhibition with kick, and the dominant population (35 out of 49; 71%) showed phasic excitation with kick. Of the 123 neurons, 24 encoded both light pulses and kick events (Fig. 4a and Supplementary Fig. 18; all summary data can be found in Supplementary Fig. 19).

As we found robust phasic electrophysiological responses to escape-related behaviours in the NAc, and observed that VTA dopamine action was causally involved in depression-related behaviour (Figs 1 and 2) and that dopamine signalling in the NAc was required for mediating escape-related behaviours (Supplementary Fig. 11b), we examined relevant circuit responses by determining whether VTA dopamine neurons modulated the neural representation of escape behaviour in the NAc. We began by distinguishing kick events occurring during light-on (VTA dopamine neuron activation) epochs from those occurring during light-off epochs. Of the 123 neurons, 14 (11%) showed phasic responses to kicks that occurred during both light-on and light-off epochs; 13 of these 14 cells similarly represented kick in both epochs (Fig. 4b; Example cell 6), and only 1 of these 14 cells differentially represented kick in the light-on epoch relative to the light-off epoch (Fig. 4b; Example cell 5). Next, we found that light activation of VTA dopamine neurons powerfully altered the encoding of kick events in two substantial populations of NAc neurons (Fig. 4b). Of the 123 neurons, 13 (11%) selectively encoded escape-related behaviour but only during the light-on (VTA dopamine neuron activation) epoch, and 16 out of 123 neurons (13%) selectively encoded escape-related behaviour but only during the light-off (baseline) epoch (Fig. 4b). Optogenetic recruitment of VTA dopamine neurons, which gives rise to antidepressed-like escape behaviour, therefore appeared to recruit a novel representation of the escape action in the NAc of freely moving rodents (Fig. 4).

Here, we have shown that selective inhibition of VTA dopamine neurons acutely induces multiple distinct depression-like behaviours, that chronic mild stress induces a lasting depression-like phenotype with multiple symptoms reversed by phasic activation of VTA dopamine neurons, that NAc dopamine (but not glutamate) receptors are required for the action of these neurons in depression-related escape behaviour, and that NAc neurons encode phasic activation of VTA dopamine neurons as well as depression-related escape behaviour. Furthermore, we have shown that the NAc representation of this depression-related behavioural action is in fact fundamentally altered by VTA dopamine neuron activation. These findings may together provide circuit-level insight into the causal dynamics of depression-related behaviour.

Certain earlier VTA recordings in depression models have shown reduced bursting that was restored after treatment with antidepressant[19], consistent with our results and the finding that attenuation of the mesocortical dopaminergic pathway may be linked to social-defeat susceptibility[20]. Conversely, other studies have instead shown increased bursting in mice susceptible to a 10-day social defeat[21,22]. Differences might stem from the models used, as chronic mild stressors could reduce dopamine neuron firing, whereas more severe stressors analogous to those employed in social defeat models could increase dopamine neuron firing[23]. Our results on depression-related behaviours are consistent with models of dopamine-mediated responses in reward-related behaviour[7,24], with VTA dopamine firing underlying anticipation or receipt of reward[2,3,6,25], with VTA GABA-neuron firing underlying aversion or anhedonia[26,27], with chemical and electrical VTA-stimulation effects on feeding, and with antidepressant effects achieved by deep brain stimulation in the NAc[17,24]. It is important to emphasize in this context that the effects of stress on the mesolimbic dopamine system are highly complex[28], as different stressors can cause opposite responses from VTA neurons depending on pre-exposure and severity[23].

Depression and its treatment are likewise exceedingly complex; for example, serotonergic pathways and agents exert antidepressant effects, and antidepressant effects of deep brain stimulation are seen in the subgenual cingulate cortex distinct from the classical mesolimbic dopamine system[29]. These results underscore the fact that psychiatric diseases defined by a constellation of different classes of symptoms can be influenced by multiple neural circuit processes. The heterogeneity of mood disorders further complicates the pinpointing of precise circuit dysfunctions mediating symptoms of depression[30]. In animal models, tests such as sucrose consumption (when depressed patients can experience either increased or decreased appetite) and the FST (which may involve transitions between active and passive coping strategies) must be interpreted with caution. However, studying targeted circuits that are well-conserved between rodents and humans, and that (as we have found) specifically cause, correct and encode diverse symptom classes of depression, will likely continue to advance our understanding of the biological underpinnings of depression and related behaviours.

METHODS

Subjects

TH::IRES-Cre homozygous male mice (Figs 1 and 2) obtained from the European Mouse Mutant Archive (mouse line EM:00254) were bred with wild-type C57BL/7 females to produce subjects. Only heterozygous TH::IRES-Cre male offspring that had been back-crossed for at least five generations were used for experiments. Animals were age matched, underwent surgery and were divided into two groups: the chronic mild stress (CMS) group and the control non-CMS group. Non-CMS animals were housed in a quiet room with a reverse 12 h light–dark cycle and given food and water *ad libitum*. CMS animals were housed separately and were subjected to standard CMS protocols; two stressors per day for 8 to 12 weeks before behavioural testing. Mice in this group experienced one stressor during the day and a different stressor during the night. Well-validated and approved standard stressors were randomly chosen from the following list so as to be unpredictable for

subjects: cage tilt on a 45° angle for 1 to 16 h; food deprivation for 12 to 16 h; white noise (http://www.simplynoise.com) for 1 to 16 h; strobe light illumination for 1 to 16 h; crowded housing (4 to 5 mice in a 10 cm × 13 cm × 13 cm plastic box with air holes) for 1 to 3 h; individual housing (separating cage-mates into single-housing cages) for 1 to 16 h ; light cycle (continuous illumination) for 24 to 36 h; dark cycle (continuous darkness) for 24 to 36 h; water deprivation for 12 to 16 h; damp bedding (200 ml water poured into sawdust bedding) for 12 to 16 h.

When not undergoing crowded housing, food deprivation or water deprivation stressors, water and food were available *ad libitum*. Experimental protocols were approved by Stanford University Institutional Animal Care and Use Committee (IACUC) and meet guidelines of the National Institutes of Health guide for the Care and Use of Laboratory Animals.

TH::Cre BAC transgenic rats (Fig. 4) were bred by mating Cre-positive founders to wild-type rats to produce TH::Cre heterozygous transgenic rats on a Long-Evans background. Only male rats aged 5 to 7 months were used for experiments. All rats underwent a 5- to 7-week chronic mild stress paradigm before behavioural testing and electrophysiological recording. Animals were subjected to the same twice-daily stressors on the same time course, except crowded housing and individual housing were both replaced with a standard restraint tube stressor in which the animal is immobilized in a cylindrical plastic tube (Braintree Scientific) for 30 to 45 min. All rats were singly housed with a 12 h standard light–dark cycle and when not undergoing water deprivation, food deprivation or restraint stress, water and food were available *ad libitum*. Experimental protocols were approved by Stanford University IACUC and meet guidelines of the NIH guide for the Care and Use of Laboratory Animals.

Virus preparation

Virus preparation was as described previously[6] with ChR2–eYFP (mice), ChR2(H134R)-eYFP (rats only), eNpHR3.0–eYFP (mice) or the eYFP alone (all) inserted between incompatible *loxP* and *lox2722* sites in reverse orientation. In all cases, the cassette was cloned into a pAAV2-MCS vector carrying the EF-1α promoter, and the woodchuck hepatitis virus post-transcriptional regulatory element (WPRE) to enhance expression. All Cre-inducible recombinant AAV vectors were packaged with AAV5 coat proteins at the University of North Carolina Vector Core. The final viral concentration was 3×10^{12} particles per ml for ChR2 virus and 1.5×10^{12} particles per ml for the eNpHR3.0 virus.

Stereotactic injection into VTA, and cannula and fibre implantation

Mice in Figs 1 and 2 were aged 2 to 4 months. These mice were deeply anaesthetized with isofluourane and placed into a stereotactic apparatus. The head was levelled using Bregma and Lambda reference points and a craniotomy was preformed. Virus was injected at 2 sites in the VTA of the right hemisphere using a 33-gauge metal needle and a 10-μl syringe controlled by an injection pump at 0.1 μl min^{-1} for 2 μl: (1 μl at anterior–posterior, −3.3; lateral–medial, 0.5; dorsal–ventral, −4.1; and 1 μl at dorsal–ventral, −4.6). The needle was left in place after injection for 10 min before slowly being withdrawn. For all mice, an

implantable fibre-optic light guide (IFL), consisting of a metal ferrule, 2.5 mm in diameter with a 200-mm thick, 5-mm long cleaved bare optic fibre (Doric Lenses) was implanted at anterior–posterior, −3.3; lateral–medial, +0.5; and dorsal–ventral, −3.9. In addition to this implant, mice used for pharmacological manipulations were also implanted with a bilateral guide cannula with a 1mm centre to centre distance for guides at coordinates (anterior–posterior, +1.2; lateral–medial, +0.5; lateral–medial, −0.5; dorsal–ventral, − 3.25), 0.5 mm above the NAc. Instant adhesive was placed between the base of the cannula and the skull, and skull fixture adhesive was used to cement the cannula to the skull.

Blue and yellow light delivery and protocols

A 200-μm patch cord was connected to the external portion of the chronically implantable optical fibre with a zirconia sleeve. Optic fibres were attached through an FC/PC adaptor to a 473-nm blue laser diode (no. BCL-473-050-M), and light pulses were generated through a stimulator (no. 33220A). For rats and mice expressing ChR2 and their eYFP controls, the light paradigm was 8 light pulses at 30 Hz every 5 s. Light-on epochs were 3 min for all assays (TST, OFT and FST) other than for anhedonia, for which the light epoch was 30 min. Optical-fibre light power from the patch cord was measured using a light sensor (S130A) and intensity calculated using a model based on empirical measurements from mammalian brain tissue for predicting irradiance values (http://www.stanford.edu/group/dlab/cgi-bin/graph/chart.php). For ChR2-transduced mice and controls, estimated light intensity at 0.5 mm from fibre tip ranged from 22.7 to 26.2 mW mm^{-2}. For yellow light stimulation in eNpHR3.0 animals and eYFP controls, a 593-nm yellow laser was used; light intensity was calculated to be from 1.9 to 4.9 mW mm^{-2}, and illumination was constant in light-on epochs. For rats, 300-μm patch cords and FC/PC cables were used with 0.37 NA fibre, and light intensity ranged from 17.0 to 23.8 mW mm^{-2}.

Pharmacological infusion of glutamate and dopamine receptor antagonists

For pharmacological experiments, drug or saline were infused in a volume of 0.4 μl through a 26-gauge stainless steel double internal cannula (PlasticsOne) that was 0.5 mm longer than the guide cannula. Each graph in Fig. 3 depicts a within-subjects matched comparison, counter-balanced for treatment order. The internal cannula was connected to a microsyringe pump by a PE20 tube. Solutions were administered at a constant rate of 100 nl min^{-1}, and the injection cannula was removed 2 min after the termination of the injection; TST was performed 10 min post infusion. For dopamine receptor antagonist experiments, 800 ng of SCH23390 per 0.4 μl per side at a concentration of 6.16 mM SCH23390 was infused for antagonism of D1-like receptors and 400 ng per 0.4 μl per side at a concentration of 2.89 mM raclopride was infused for D2-like receptor antagonism. For glutamate receptor antagonism, 3 μg per 0.4 μl per side, at a concentration of 22.3 mM for NBQX and 3 μg per 0.4 μl per side at a concentration of 38.04 mM for AP5 was used to antagonize AMPA (α-amino-3-hydroxy-5-methyl-4-isoxazole propionic acid) and NMDA (*N*-methyl-D-aspartate) receptors, respectively. Each animal was experimentally tested using the TST, once post drug infusion and once post saline infusion, with order counterbalanced; the two tests were carried out in different contexts on different days.

Immunohistochemistry

To determine the specificity of eNpHR3.0–eYFP expression in dopamine neurons, TH::IRES-Cre mice transduced with the double-floxed AAV encoding eNpHR3.0–eYFP were anaesthetized and transcardially perfused with PBS followed by 4% paraformaldehyde (PFA) dissolved in PBS. Brains were removed and post-fixed in PBS containing 4% PFA overnight at 4 °C, and subsequently immersed in a cryoprotectant consisting of PBS containing 30% sucrose until settling (~48 h at 4 °C). Coronal brain sections (40 μm) were collected and washed in PBS; blocking solution, primary and secondary solutions contained 0.3% Triton X-100 (PBST) and 3% normal donkey serum dissolved in PBS. Localization of dopamine cell bodies and fibres was confirmed by labelling with chicken anti-tyrosine hydroxylase antibody (1:300). Cell bodies were identified using the 4′,6-diamidino-2-phenylindole (DAPI) stain (1:50,000). Transduction efficiency was quantified using a confocal microscope by comparing the eYFP cells with TH-immunoreactive cells.

Behavioural testing

For animals undergoing CMS, behavioural testing occurred after 8 to 12 weeks of CMS for mice (or 8 to 12 weeks of no CMS for non-CMS controls) or 4 to 6 weeks of CMS for rats. For NpHR animals and eYFP controls, behavioural testing occurred at least 1 month post surgery. All behaviour was conducted during the dark cycle (07:00 to 19:00).

Open field test

The open-field test was conducted in an open plastic chamber (50 cm long, 50 cm wide and 40 cm deep). Mice were plugged into a patch cord connecting to the external portion of the chronically implanted optical fibre, individually placed in the centre of the chamber and allowed to freely explore for 12 min. Velocity of the animal in the field was measured using an automated video-tracking system (Viewer II, BiObserve). Measurement began immediately after placement in the chamber. Light stimulation occurred for minutes 3 to 6 and 9 to 12 only. Although no difference was detected, any trend towards subtly decreased locomotion in the eNpHR3.0 group after illumination in the OFT would still be consistent with a depression-related phenotype, as related motor changes are clinically observed as psychomotor retardation and/or reduced motivation to explore[31].

Tail-suspension test

Mice were plugged into a patch cord and the tail was placed between two strips of autoclave labelling tape. The end of one strip of tape was then secured to a horizontal bar 40 cm from the ground, ensuring that the animal could not make other contact or climb during the assay. Video recording was started 90 s from the time that the animal was inverted and taped; light stimulation was between minutes 3 to 6 of the assay. Time spent struggling was measured by blind scoring each minute of video material after the testing was completed, and was reported in seconds for each minute of the assay.

Sucrose-preference test

TH::Cre males transduced with ChR2–eYFP or eNpHR3.0–eYFP were tested alternately with their respective eYFP-only controls. Animals were water-restricted overnight before

exposure to the lickometer. A Med Associates operant chamber was used to count every tongue contact made ('licks') with either the 1% sucrose in water solution or the water alone. Bottle side and animal group tested were counterbalanced among chambers. In the 90-min test, the first 30 min of the assay were used to collect a baseline sucrose preference. Over the next 30 min of the session (minutes 30–60), light delivery occurred through a jacketed patch cord, with blue light for ChR2 animals and eYFP controls (CMS and non-CMS groups) at 8 pulses at 30 Hz every 5 s, or constant yellow light for the eNpHR3.0 animals and their eYFP controls at the same light intensities used for TST assays. The last 60 to 90 min of the test was again a no-light post light delivery measure of sucrose preference. To ensure that all animals had consumed liquid from both spouts, identified the location of the sucrose and water spouts (counter-balanced across animals), and familiarized themselves with the placement of the bottles, light delivery between 30 and 60 min only occurred if both spouts had been used in the first 30-min baseline epoch. If the animal failed to lick at either spout during the first epoch (indicating that the mouse did not discover the spout and identify the solution within), the test was aborted at 30 min, the animal did not receive any light and the test was repeated on a different day.

In vivo NAc electrophysiology

TH::Cre rats received AAV5-EF1a-DIO-ChR2–eYFP to enable expression before CMS. Two small craniotomies were drilled unilaterally over the VTA at the following coordinates: anterior–posterior, −5.4 and −6.2; lateral–medial, ± 0.7. A bevelled 33-gauge needle was used to deliver 1.0 μl of virus at 2 depths in each hole (dorsal–ventral, −8.2 and −7.0; all coordinates from skull surface) for a total of 4.0 μl per animal. Each 1.0 μl of virus was infused at a speed of 100 nl min^{-1} using a syringe pump; the virus infuser was left in place for an additional 10 min after each injection before being removed slowly. After the CMS protocol described above, these animals had a 24-wire fixed electrode array implanted into the medial shell of the NAc (anterior–posterior, 1.6; lateral–medial, 1.3; dorsal–ventral, −7.5). A third burr hole was drilled (anterior–posterior, −5.8; lateral–medial, ± 0.7; dorsal–ventral −7.5) for the insertion of an implantable optical fibre targeted just dorsal to the VTA. Ground wires were implanted at a depth of approximately 2 mm lateral to the optical fibre. After behavioural and recording experiments, electrolytic lesions were created just before sacrifice to allow histological identification of electrode-tip location.

Forced swim test

On day 1, a 15-min pre-test swim was conducted for each animal, and on day 2 rats were plugged into a patch cord and a HS-27 pre-amplifier head stage with 24 electrode channels and 3 reference channels. The patchcord and HS-27 tether were waterproofed with a latex tube before being connection. Immediately after a 5-min recording in the home cage and a 12-min OFT, the rat was placed into a cylindrical tank of water (25 to 26 °C), in which the animal could not touch the bottom of the tank. Minutes 6 to 51 were used for analysis of neural data. Light stimulation occurred during minutes 12 to 15, 21 to 24, 30 to 33, 39 to 42 and 48 to 51, to create an alternating 6 min off, 3 min on light-stimulation paradigm. Magnetic induction was used to provide a high temporal-resolution readout; swimming activity (referred to as 'kicks' or 'kick events') was timed and quantified with a coil and a hind-paw magnet to give a continuous analogue signal. This continuous signal was then

thresholded at 3 standard deviations from the mean for all rats through both light-on and light-off epochs in the FST.

Analysis of *in vivo* awake-behaving NAc electrophysiological recordings

To test the relevance of phasic-firing-rate changes for individual neurons in relation to either light-pulse onsets or kick-signal threshold crossings (Fig. 4), two time windows relative to the event time were used. For the statistical analyses of neural responses to the first light pulse in each 8-pulse train and kick signals (all trials were included unless otherwise stated), a baseline window was compared to a response window for each reference event. For the reference event referred to as 'light', the event was the onset of the first light pulse in each 8-pulse train occurring every 5 s; we selected a baseline window from $t = -3$ s to -2 s, and selected the response window that initiated after first light-pulse onset and spanned from $t =$ 0 s to 1 s. For kick events (animal-initiated rather than experimenter-initiated), we used a baseline window further from the event onset given the variable inter-event interval latency; −4 s to −2 s was used as a measure of baseline firing rate for all kick events, and a response window from −0.5 s to 0.5 s was used as a measure of the response. Bin size for rate calculations was 200 ms. For all phasic responses discussed in this study, the fractional change in the average firing rate between the baseline and response window was computed across all event occurrences (for events, the number of events ranged from 1,971 to 4,718 events), and the significance of this change was determined by its percentile within a non-parametric bootstrap distribution estimated using 500 random circular permutations of spike times relative to events times, in which P values of less than 0.05 were considered significant responses. For all classes of reference events, the number of significantly modulated neurons statistically exceeded the expected number of false positives given multiple comparisons (95% confidence interval of 2 to 11 false positives occurring, binomial test, $n = 123$, $\alpha = 0.05$). Mean firing-rate changes are indicated in Supplementary Fig. 17 and described in the main text.

Extended, counterbalanced open-field test

For data shown in Supplementary Fig. 3, the open-field test was conducted in an open plastic chamber (50 cm long, 50 cm wide and 40 cm deep). Mice were plugged into a patch cord connecting to the external portion of the chronically implanted optical fibre, individually placed in the centre of the chamber and allowed to freely explore for 30 min. Velocity and distance travelled were measured using an automated video-tracking system (Viewer II, BiObserve). Measurements began immediately after animals were placed in the chamber. For one-half of each group, light stimulation occurred for minutes 0 to 10 and 20 to 30, and for the remaining half, light stimulation occurred from minutes 10 to 20.

In vivo VTA electrophysiology

Adult (>300-g) male Long Evans rats underwent either the rat CMS ($n = 5$) protocol described above or spent equal time in a quiet, low-traffic animal housing facility with water and food *ad libitum* (non-CMS; $n = 4$). In the last week of the treatment, animals were deeply anaesthetized and implanted with a 12- or 24-wire array into the VTA (anterior–posterior, −5.8; lateral–medial, ± 0.7; dorsal–ventral, −8.2) as described with NAc recording

subjects. After recovery and before recording, subjects were connected to an HS-27 (Neuralynx), returned to the home cage and given 45 min to habituate to the tether. After these 45 min, approximately 60-min recordings were carried out in the home cage for each animal. After recording experiments, electrolytic lesions were created just before animals were euthanized to enable histological identification of electrode-tip location (Supplementary Fig. 10).

Burst-firing analysis

Bursts were defined as beginning when 2 spikes occurred with an inter-spike interval of less than 80 ms and as ending when the inter-spike interval was greater than 135 ms, as described by previously[32] (see also refs 33, 34). Spike sorting was performed using the Offline Sorter (Plexon) and burst analyses were calculated using NeuroExplorer (Plexon), with the parameters specified above, and the minimum number of spikes in a burst was set at two.

Supplementary Material

Refer to Web version on PubMed Central for supplementary material.

Acknowledgments

We thank T. Davidson, S. Pak, C. Ramakrishnan, L. Grosenick, Z. Chen and the members of the Deisseroth Laboratory for support. I.B.W. was supported by the Helen Hay Whitney Foundation; K.M.T was supported by NRSA fellowship F32 MH880102 and the JPB Foundation; K.R.T., M.R.W. and K.D. are NARSAD grant awardees. K.D. was supported by the Wiegers Family Fund and by the NIMH, the NIDA, the DARPA REPAIR Program, the Keck Foundation, the McKnight Foundation, the Gatsby Charitable Foundation, the Snyder Foundation, the Woo Foundation and the Albert Yu and Mary Bechman Foundation. All tools and methods described are distributed and supported freely (http://www.optogenetics.org).

References

1. Kessler RC, Chiu WT, Demler O, Walters EE. Prevalence, severity, and comorbidity of 12-month DSM-IV disorders in the national comorbidity survey replication. Arch. Gen. Psychiatry. 2005; 62:617–627. [PubMed: 15939839] 2005; 62:709. erratum.
2. Schultz W, Dayan P, Montague PR. A neural substrate of prediction and reward. Science. 1997; 275:1593–1599. [PubMed: 9054347]
3. Witten IB, et al. Recombinase-driver rat lines: tools, techniques, and optogenetic application to dopamine-mediated reinforcement. Neuron. 2011; 72:721–733. [PubMed: 22153370]
4. Willner P, Muscat R, Papp M, Stamford J, Kruk Z. Dopaminergic mechanisms in an animal model of anhedonia. Eur. Neuropsychopharmacol. 1991; 1:295–296.
5. Roitman MF, Wheeler RA, Wightman RM, Carelli RM. Real-time chemical responses in the nucleus accumbens differentiate rewarding and aversive stimuli. Nature Neurosci. 2008; 11:1376–1377. [PubMed: 18978779]
6. Tsai H-C, et al. Phasic firing in dopaminergic neurons is sufficient for behavioral conditioning. Science. 2009; 324:1080–1084. [PubMed: 19389999]
7. Wise RA. Dopamine,learningandmotivation. NatureRev.Neurosci. 2004; 5:483–494.
8. Koob G. Hedonic valence, dopamine and motivation. Mol. Psychiatry. 1996; 1:186. [PubMed: 9118342]
9. Ikemoto S, Panksepp J. The role of nucleus accumbens dopamine in motivated behavior: a unifying interpretation with special reference to reward-seeking. Brain Res. Brain Res. Rev. 1999; 31:6–41. [PubMed: 10611493]

10. Nestler EJ, Carlezon WA Jr. The mesolimbic dopamine reward circuit in depression. Biol. Psychiatry. 2006; 59:1151–1159. [PubMed: 16566899]
11. Lammel S, et al. Input-specific control of reward and aversion in the ventral tegmental area. Nature. 2012
12. Porsolt RD, Le Pichon M, Jalfre M. Depression: a new animal model sensitive to antidepressant treatments. Nature. 1977; 266:730–732. [PubMed: 559941]
13. Willner P, Muscat R, Papp M. Chronic mild stress-induced anhedonia: a realistic animal model of depression. Neurosci. Biobehav. Rev. 1992; 16:525–534. [PubMed: 1480349]
14. Strekalova T, Spanagel R, Bartsch D, Henn FA, Gass P. Stress-induced anhedonia in mice is associated with deficits in forced swimming and exploration. Neuropsychopharmacology. 2004; 29:2007–2017. [PubMed: 15266352]
15. Cryan JF, Mombereau C, Vassout A. The tail suspension test as a model for assessing antidepressant activity: Review of pharmacological and genetic studies in mice. Neurosci. Biobehav. Rev. 2005; 29:571–625. [PubMed: 15890404]
16. Fields HL, Hjelmstad GO, Margolis EB, Nicola SM. Ventral tegmental area neurons in learned appetitive behavior and positive reinforcement. Annu. Rev. Neurosci. 2007; 30:289–316. [PubMed: 17376009]
17. Bewernick BH, et al. Nucleus accumbens deep brain stimulation decreases ratings of depression and anxiety in treatment-resistant depression. Biol. Psychiatry. 2010; 67:110–116. [PubMed: 19914605]
18. Berman RM, et al. Antidepressant effects of ketamine in depressed patients. Biol. Psychiatry. 2000; 47:351–354. [PubMed: 10686270]
19. Friedman A, Friedman Y, Dremencov E, Yadid G. VTA dopamine neuron bursting is altered in an animal model of depression and corrected by desipramine. J. Mol. Neurosci. 2008; 34:201–209. [PubMed: 18197479]
20. Tanaka K, et al. Prostaglandin E2-mediated attenuation of mesocortical dopaminergic pathway is critical for susceptibility to repeated social defeat stress in mice. J. Neurosci. 2012; 32:4319–4329. [PubMed: 22442093]
21. Cao J-L, et al. Mesolimbic dopamine neurons in the brain reward circuit mediate susceptibility to social defeat and antidepressant action. J. Neurosci. 2010; 30:16453–16458. [PubMed: 21147984]
22. Krishnan V, et al. molecular adaptations underlying susceptibility and resistance to social defeat in brain reward regions. Cell. 2007; 131:391–404. [PubMed: 17956738]
23. Valenti O, Gill KM, Grace AA. Different stressors produce excitation or inhibition of mesolimbic dopamine neuron activity: response alteration by stress pre-exposure. Eur. J. Neurosci. 2012; 35:1312–1321. [PubMed: 22512259]
24. Ikemoto S, Wise RA. Mapping of chemical trigger zones for reward. Neuropharmacology. 2004; 47(Suppl. 1):190–201. [PubMed: 15464137]
25. Cohen JY, Haesler S, Vong L, Lowell BB, Uchida N. Neuron-type-specific signals for reward and punishment in the ventral tegmental area. Nature. 2012; 482:85–88. [PubMed: 22258508]
26. Tan KR, et al. GABA neurons of the VTA drive conditioned place aversion. Neuron. 2012; 73:1173–1183. [PubMed: 22445344]
27. van Zessen R, Phillips JL, Budygin EA, Stuber GD. Activation of VTA GABA neurons disrupts reward consumption. Neuron. 2012; 73:1184–1194. [PubMed: 22445345]
28. Lemos JC, et al. Severe stress switches CRF action in the nucleus accumbens from appetitive to aversive. Nature. http://dx.doi.org/10.1038/nature11436.
29. Mayberg HS, et al. Deep brain stimulation for treatment-resistant depression. Neuron. 2005; 45:651–660. [PubMed: 15748841]
30. Tye KM, Deisseroth K. Optogenetic investigation of neural circuits underlying brain disease in animal models. Nature Rev. Neurosci. 2012; 13:251–266. [PubMed: 22430017]
31. Lemke MR, Wendorff T, Mieth B, Buhl K, Linnemann M. Spatiotemporal gait patterns during over ground locomotion in major depression compared with healthy controls. J. Psychiatr. Res. 2000; 34:277–283. [PubMed: 11104839]

32. Ungless MA, Magill PJ, Bolam JP. Uniform inhibition of dopamine neurons in the ventral tegmental area by aversive stimuli. Science. 2004; 303:2040–2042. [PubMed: 15044807]

33. Grace AA, Bunney BS. The control of firing pattern in nigral dopamine neurons: burst firing. J. Neurosci. 1984; 4:2877–2890. [PubMed: 6150071]

34. Freeman AS, Bunney BS. Activity of A9 and A10 dopaminergic neurons in unrestrained rats: further characterization and effects of apomorphine and cholecystokinin. Brain Res. 1987; 405:46–55. [PubMed: 3032350]

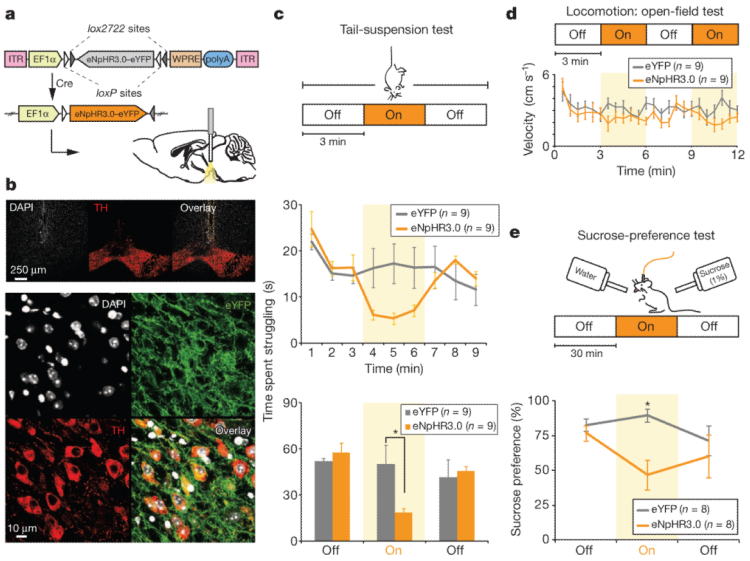

Figure 1. Selective inhibition of VTA dopamine neurons induces a depression-like phenotype

a, Cre-dependent AAV. **b,** Confocal images of midbrain dopamine neurons. Orange dotted lines, location of fibre optic. Bottom, images of VTA neurons directly below fibre track. **c,** Photoinhibition of VTA dopamine neurons acutely reduces escape-related behaviour. Two-way ANOVA demonstrates the group-by-light epoch interaction (interaction of the experimental-group factor and light-condition factor in the test), $F_{4,38} = 3.95$, $P = 0.00089$; Bonferroni post-hoc test shows reduced struggling in the eNpHR3.0 group relative to the eYFP group, $^*P < 0.05$. Error bars, s.e.m. **d,** Inhibition of VTA dopamine neurons does not produce a significant difference in open-field locomotion; two-way ANOVA did not demonstrate a significant group-by-light epoch interaction, $F_{3,48} = 1.76$, $P = 0.17$. Error bars, s.e.m. **e,** Schematic and results of the 90-min sucrose-preference test. Photoinhibition of VTA dopamine neurons acutely reduces sucrose preference; two-way ANOVA revealed that opsin expression has a significant effect, $F_{1,42} = 6.31$, $P = 0.016$; Bonferroni post-hoc test revealed significant differences between groups only in the light-on epoch, $^*P < 0.05$. Error bars, s.e.m. Off, light off; On, light on; WPRE; woodchuck hepatitis virus post-transcriptional regulatory element.

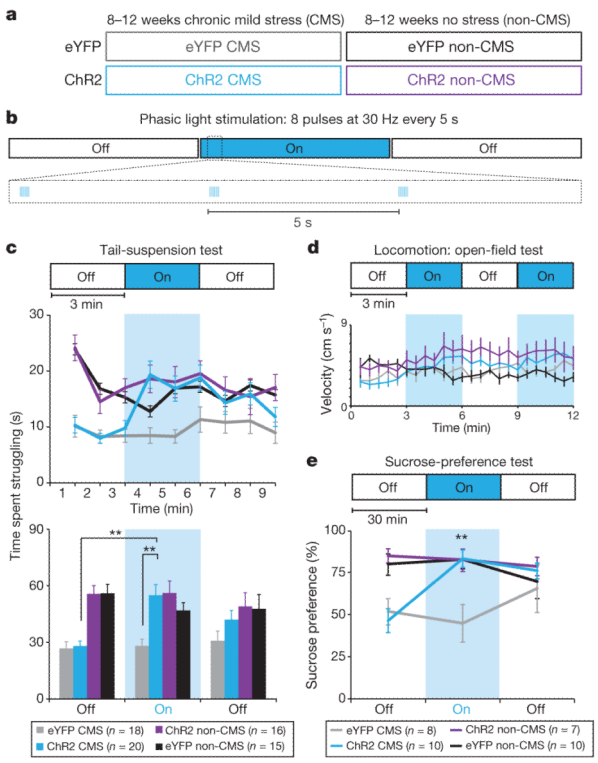

Figure 2. Temporally sparse phasic photoactivation of VTA dopamine neurons rescues stress-induced depression-like phenotype

a, Experimental groups. **b,** Schematic of illumination pattern; 473-nm light used to elicit phasic bursts of activity in ChR2-expressing VTA dopamine neurons. **c,** Phasic illumination of VTA dopamine neurons rescues stress-induced reduction in struggling on TST in ChR2 CMS but not eYFP CMS mice (**$P < 0.001$; eYFP CMS = 26.8 s ± 3.5 s; ChR2 CMS = 28.0 s ± 2.7 s; ChR2 non-CMS = 55.63 s ± 4.4 s; eYFP non-CMS = 56.0 s ± 4.7 s). Two-way ANOVA revealed a significant group-by-light epoch interaction ($F_{6,134} = 6.04$, $P < 0.0001$) and a significant influence of experimental condition on performance as revealed by one-way ANOVA ($F_{3,67} = 6.20$, $P = 0.0009$; Bonferroni post-hoc test). Error bars, s.e.m. **d,** Illumination parameters, as used in the TST, did not change locomotor activity in the open field, with no significant group-by-epoch interaction in two-way ANOVA ($F_{9,152} = 0.99$, $P = 0.4493$), and no detectable differences revealed by Bonferroni post-hoc tests on the same timescale. Error bars, s.e.m. **e,** Phasic activation of VTA dopamine neurons rescued the stress-induced decrease in sucrose preference in ChR2 CMS, but not eYFP CMS mice; one-way ANOVA, Dunn's post-hoc test comparing baseline to light-on epoch, $P < 0.01$ for ChR2 CMS mice, $P = 0.2851$ for eYFP CMS mice. Two-way ANOVA revealed a significant group-by-light epoch interaction ($F_{6,62} = 4.33$, $P = 0.001$), and a significant influence of experimental condition on performance was revealed by one-way ANOVA ($F_{3,31} = 3.40$, $P = 0.0299$); **$P < 0.01$ for ChR2 CMS mice. Error bars, s.e.m.

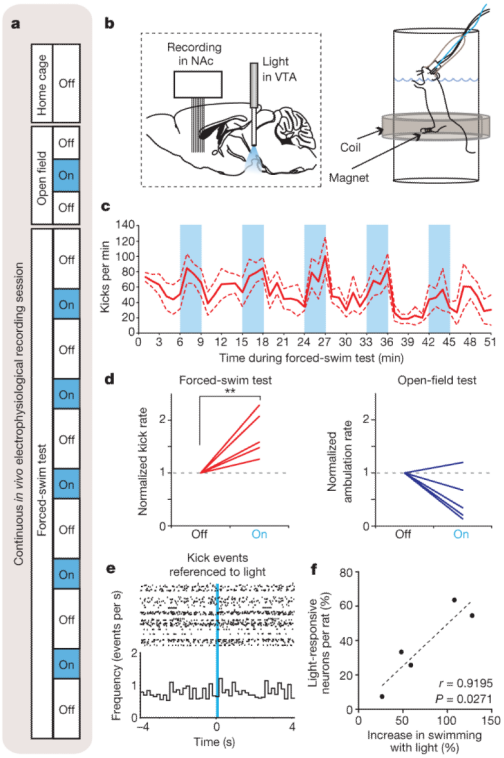

Figure 3. Phasic activation of VTA dopamine neurons modulates escape-related behaviour in TH::Cre rats

a, *In vivo* electrophysiology sessions. **b,** Integration of recordings in the NAc, illumination of ChR2-expressing VTA dopamine neurons, and precision measurement of swimming behaviour in five TH::Cre rats treated with CMS. **c,** Light-induced modulation of swimming; phasic illumination of ChR2-expressing VTA dopamine neurons increases escape behaviour of TH::Cre rats in FST. Thick red line, mean kick rate; dotted lines, s.e.m. **d,** Phasic illumination of ChR2-expressing VTA dopamine neurons increases kick rate in FST (paired *t*-test; ***P* = 0.0088; mean increase in kick rate of 73.9% ± 21.2% relative to light-off epochs) but not ambulation rate in OFT (mean decrease of 60.2% ± 22.9%; mean ± s.e.m.). **e,** Peri-event raster histogram showing kick events referenced to the train of 8 light pulses at 30 Hz every 5 s (blue); kick events are not time-locked to light pulses (bin width of 0.175 s for all histograms). **f,** Scatter-plot relating the degree to which behaviour of each rat was modulated by light-driven VTA dopamine neuron activation, to the proportion of all light-responsive units recorded from the same subject (Pearson's correlation Test, *P* = 0.0271, *r* = 0.9195).

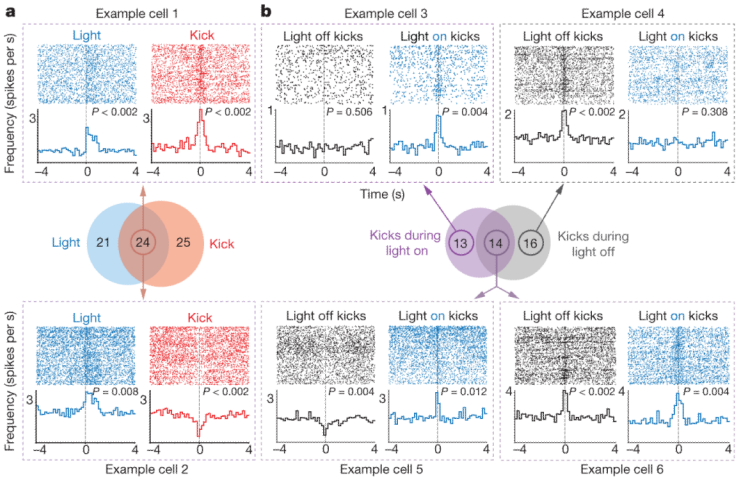

Figure 4. Phasic activation of VTA dopamine neurons modulates NAc encoding of escape-related behaviour

Recording of 123 NAc neurons from 5 CMS TH::Cre rats expressing ChR2 in VTA dopamine neurons. **a,** Peri-event raster histograms for representative neurons showing phasic excitation associated with both light pulses and kick events (Example cell 1; 15 out of 24 cells) or for representative neurons showing different phasic responses with light pulses versus kick events (Example cell 2; 9 out of 24 cells). **b,** Peri-event raster histograms for representative neurons that selectively encoded kick events during either the light-on epoch (Example cell 3; 13 cells) or the light-off epoch (Example cell 4; 16 cells), or encoded kick events in both light-on and light-off epochs differentially (Example cell 5; 1 out of 14 cells) or similarly (Example cell 6; 13 out of 14 cells).